2009 American Control Conference
Hyatt Regency Riverfront, St. Louis, MO, USA
June 10-12, 2009

Partial Integrated Guidance and Control of Surface-to-Air Interceptors for High Speed Targets

Radhakant Padhi, Charu Chawla, Priya G. Das and Abhiram Venkatesh

Abstract— **An important limitation of the existing IGC algorithms, is that they do not explicitly exploit the inherent time scale separation that exist in aerospace vehicles between rotational and translational motions and hence can be ineffective. To address this issue, a two-loop partial integrated guidance and control (PIGC) scheme has been proposed in this paper. In this design, the outer loop uses a recently developed, computationally efficient, optimal control formulation named as model predictive static programming. It gives the commanded pitch and yaw rates whereas necessary roll-rate command is generated from a roll-stabilization loop. The inner loop tracks the outer loop commands using the Dynamic inversion philosophy. Uncommonly, Six-Degree of freedom (Six-DOF) model is used directly in both the loops. This intelligent manipulation preserves the inherent time scale separation property between the translational and rotational dynamics, and hence overcomes the deficiency of current IGC designs, while preserving its benefits. Comparative studies of PIGC with one loop IGC and conventional three loop design were carried out for engaging incoming high speed target. Simulation studies demonstrate the usefulness of this method.**

Keywords- **partial integrated guidance and control, high speed targets, model predictive static programming, dynamic inversion**

I. INTRODUCTION

Stringent performance demands are expected for new-generation interceptors to engage high speed targets, especially in defense applications. This is a challenging problem because of several reasons, which include high relative velocity (and hence very less time availability), high altitude engagement and hence limited turning capability (due to reduced dynamic pressure), hit-to-kill capability (i.e. zero miss distance) demand etc. The trajectory of an interceptor is typically divided into three segments consisting of lift-off, mid-course and terminal phases respectively [1]. Out of these three phases, the terminal homing is a very crucial phase. In this phase the interceptor locks on to the target directly (through a seeker) and the guidance and control algorithms are designed in such a way that the residual errors of the prior phases get corrected to achieve the minimum miss distance. However, conventional separated guidance and control design may not achieve this objective.

Radhakant Padhi, Asst. Professor (Contact author), is with the Department of Aerospace Engineering, Indian Institute of Science, Bangalore, India. Email: padhi@aero.iisc.ernet.in

Charu Chawla and Priya G. Das, Graduate students, are with the Department of Aerospace Engineering, Indian Institute of Science, Bangalore, India.

Abhiram Venkatesh, Formerly Project Asst., was with the Department of Aerospace Engineering, Indian Institute of Science, Bangalore, India.

The conventional guidance and control philosophy works in three loops. In the outermost loop, a point mass engagement model is considered to generate lateral acceleration (Latax) commands for achieving minimum miss distance. These latax commands are then converted into equivalent body rates in an intermediate loop, which are tracked by the inner most loop [2]. However, whenever a loop structure is followed, it introduces time lags between the inner and outer loops. In case of conventional engagements the target usually moves slowly and hence the time availability is relatively large. In such a situation this three-loop structure usually turns out to be sufficient. However, in case of incoming high speed targets (like ballistic missiles) the time availability is quite less (especially in the terminal phase). Both the guidance and autopilot loops are decoupled and hence it achieves lethality in a limited sense. Moreover, three loop design may demand higher maneuverability, which subsequently may lead to control saturation.

To overcome the deficiencies of the conventional three loop design, integrated guidance and control design (IGC) ideas have been proposed in the recent literature. In this design philosophy, attempt is made to achieve the objectives using the full nonlinear Six-DOF interceptor dynamics in a single unified (single loop) framework. Techniques like feedback linearization [2], State Dependent Riccati Equation (SDRE) technique [3], etc. have been applied in the IGC framework.

Existing IGC algorithms do not explicitly exploit the inherent time scale separation that exist in aerospace vehicles between rotational and translational motions. Hence, such an algorithm can become ineffective unless the engagement geometry is close to the collision triangle. From our numerical experiments on published ideas of IGC, we observed that the control surface deflections directly respond to the translational error correction demands, which leads to instability of the rotational dynamics. A close examination reveals that the control surface deflections (which are located at the tail of the interceptor) can create only minor forces, whereas they create large moments due to a long moment arms from the center of gravity. Hence, they are very ineffective in translational error correction directly, whereas they can be very effective in turning the vehicle. Hence for any guidance and control algorithm (including IGC) to be successful, one must exploit the time scale separation that exist in aerospace vehicles between faster rotational dynamics and slower translational dynamics.

To address the deficiency of existing IGC designs, a two-loop partial integrated guidance and control (PIGC) structure

978-1-4244-4524-0/09/$25.00 ©2009 AACC

is proposed in this paper. In this design, the commanded pitch and yaw rates are directly generated from an outer loop optimal control formulation, which is solved in a computationally efficient manner using the recently-developed model predictive static programming (MPSP) technique [4]. The necessary roll-rate command is generated from a roll-stabilization loop. The inner loop generates the necessary control using the Dynamic inversion (DI) philosophy. Uncommonly, in both the loops the Six-DOF interceptor model is used directly. Six-DOF simulation studies have been carried out in three dimentional environment to demonstrate the usefulness of this method.

II. System Model

The whole system is defined by Six-DOF interceptor model and 3-DOF target model. The equations are derived in fin and inertial frame.

A. Interceptor Model

A general nonlinear system of the interceptor can be defined as

$$\dot{X} = f(X, U_\delta) \tag{1}$$

where

$$X \triangleq [u\ v\ w\ p\ q\ r\ x_m\ y_m\ z_m\ \dot{x}_m\ \dot{y}_m\ \dot{z}_m\ q_1\ q_2\ q_3\ q_4\ \zeta]^T \tag{2}$$

$$U_\delta \triangleq [\delta_r\ \ \delta_p\ \ \delta_y]^T \tag{3}$$

The elaborated plant model can be written in the following form:

$$\begin{bmatrix} \dot{u} \\ \dot{v} \\ \dot{w} \end{bmatrix} = \begin{bmatrix} vr - wq - \frac{QSC_D}{m} - Q_{11}g \\ wp - ur + \frac{QSC_{NBN}}{m} - \frac{QSC_{N_\delta}\delta_y}{m} - \frac{(Q_{21}+Q_{31})g}{\sqrt{2}} \\ uq - vp + \frac{QSC_{NAN}}{m} - \frac{QSC_{N_\delta}\delta_p}{m} - \frac{(Q_{31}-Q_{21})g}{\sqrt{2}} \end{bmatrix} \tag{4}$$

$$\begin{bmatrix} \dot{p} \\ \dot{q} \\ \dot{r} \end{bmatrix} = \begin{bmatrix} \frac{1}{I_{XX}}\left(-QSdC_{R_M} - QSdC_{l_\xi}\delta_r + \frac{QSd^2C_{L_P}p}{2V_m} \right) \\ \frac{1}{I_{YY}}\left(QSdC_{MXCGA} - QSC_{N_\delta}(X_{CP_\delta} - X_{CG})\delta_p \right. \\ \qquad \left. -(I_{XX} - I_{ZZ})pr + \frac{QSd^2C_{M_Q}q}{2V_m} \right) \\ \frac{1}{I_{ZZ}}\left(QSdC_{MXCGB} - QSC_{N_\delta}(X_{CP_\delta} - X_{CG})\delta_y \right. \\ \qquad \left. -(I_{YY} - I_{XX})pq + \frac{QSd^2C_{N_R}r}{2V_m} \right) \end{bmatrix} \tag{5}$$

$$\begin{bmatrix} \dot{q}_1 \\ \dot{q}_2 \\ \dot{q}_3 \\ \dot{q}_4 \end{bmatrix} = \begin{bmatrix} \frac{1}{2}(q_4 p - q_3 q + q_2 r) \\ \frac{1}{2}(q_3 p - q_4 q + q_1 r) \\ \frac{1}{2}(-q_2 p + q_1 q + q_4 r) \\ \frac{1}{2}(-q_1 p - q_2 q - q_3 r) \end{bmatrix} \tag{6}$$

$$\dot{\zeta} \quad = \quad p \tag{7}$$

where, u, v, w are the interceptor velocity components and p, q, r are the actual body rates both defined in fin frame. ζ is the roll angle. q_1, q_2, q_3, q_4 are the quaternions which defines the attitude of the interceptor [1]. x_m, y_m, z_m defines the position coordinates of the interceptor in the inertial frame. The position rates in inertial frame are given by

$$\begin{bmatrix} \dot{x}_m \\ \dot{y}_m \\ \dot{z}_m \end{bmatrix} = T_{IB}^{-1} \begin{bmatrix} u_b \\ v_b \\ w_b \end{bmatrix} \tag{8}$$

In (8) u_b, v_b, w_b are the interceptor velocity components in body frame and T_{IB} is the time varying transformation matrix between inertial and body coordinate system, given by

$$T_{IB} = \begin{bmatrix} Q_{11} & Q_{12} & Q_{13} \\ Q_{21} & Q_{22} & Q_{23} \\ Q_{31} & Q_{32} & Q_{33} \end{bmatrix} \tag{9}$$

where the elements of the matrix are obtained through quaternions (q_1, q_2, q_3, q_4) [1]. The inertial acceleration of the interceptor is given by

$$\begin{bmatrix} \ddot{x}_m \\ \ddot{y}_m \\ \ddot{z}_m \end{bmatrix} = T_{IF}^{-1} \begin{bmatrix} \dot{u} - (vr - wq) \\ \dot{v} - (wp - ur) \\ \dot{w} - (uq - vp) \end{bmatrix} \tag{10}$$

where $T_{IF} = T_{BF} T_{IB}$ is the transformation matrix from inertial to fin frame. In this transformation, T_{BF} is the constant transformation matrix between body frame to fin frame. Fin frame is achieved by a $\frac{\pi}{4}$ rotation of body frame along positive X_b-axis, pointing in the direction of nose of the interceptor. Some of the parameters used in the model are Q, the dynamic pressure, V_m, the total interceptor velocity, S, the reference area, m, the mass of the interceptor, d, the diameter, g, the acceleration due to gravity and I_{xx}, I_{yy}, I_{zz} the moment of inertia about body axes respectively. The aerodynamic force and moment coefficients are evaluated in fin frame. C_D is the drag coefficient, C_{NAN} is the pitch and C_{NBN} is the yaw force coefficient respectively. $C_{N\delta}$ is the tail normal force coefficient per unit δ per pair, C_{R_M} is the rolling moment coefficient, C_{l_ξ} is the roll moment control coefficient per unit roll deflection, C_{L_P}, C_{M_Q} and C_{N_R} are damping derivatives, C_{MXCGA} and C_{MXCGB} are pitching and yawing moment coefficients respectively. X_{CP_δ} is the tail moment arm (with respect to nose), X_{CG} is the axial position of center of gravity from nose (in meters). The necessary control U_δ is generated through fin (control surfaces) deflections.

B. Target Model

The 3-DOF model of target in inertial frame based on flat earth assumptions is used. Target is not maneuvering and hence follows a straight line flight path.

$$\begin{bmatrix} \dot{V}_t \\ \dot{\psi}_t \\ \dot{\gamma}_t \\ \dot{x}_t^I \\ \dot{y}_t^I \\ \dot{z}_t^I \end{bmatrix} = \begin{bmatrix} \frac{-D}{m_t} - gsin(\gamma_t) \\ 0 \\ \frac{-gcos(\gamma_t)}{V_t} \\ V_t sin(\gamma_t) \\ V_t sin(\psi_t) cos(\gamma_t) \\ V_t cos(\gamma_t) cos(\psi_t) \end{bmatrix} \tag{11}$$

where D is the drag (aerodynamic force), m_t is the mass of the target, V_t is the total velocity of the target, γ_t is the flight path angle of the target, ψ_t is the heading angle of the target and $x_t^I\ y_t^I\ z_t^I$ are the position coordinates of the target in inertial frame.

C. Design Philosophy of PIGC

In PIGC, the guidance loop uses the translational dynamics to generate the commanded pitch and yaw rates which serves the command for the DI loop. The necessary roll-rate command is generated from a roll-stabilization loop. In DI loop, the commanded body rates are tracked to generate the necessary fin deflections which will drive in meeting the objective of minimum miss distance as shown in Fig.1. The objective of almost zero miss distance is achieved by

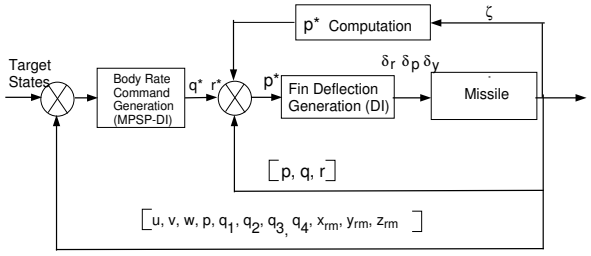

Fig. 1. Block Diagram of PIGC scheme

minimizing the relative error in position and velocity in y and z direction in fin frame with no control authority in X direction. To visualize the combined effect of guidance and

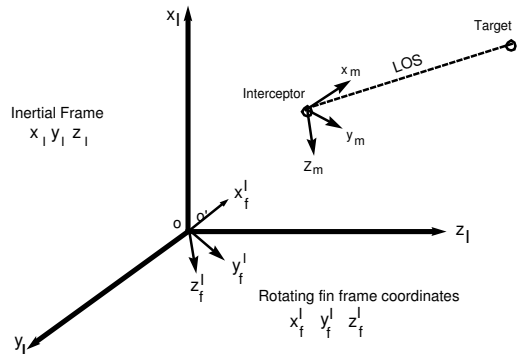

Fig. 2. Engagement Geometry in Rotating fin frame

control, transition between three reference frames namely, body frame, inertial frame and fin frame is considered in the design. The origin of the body coordinate frame is assumed to be at the interceptor center of gravity. The inertial coordinates are defined by earth fixed inertial frame. Since the interceptor seeker defines the target position relative to the interceptor body coordinates, it is desirable to define the interceptor and target position in a coordinate system parallel to the instantaneous interceptor fin axes with the origin coinciding with the origin of the inertial frame as shown in Fig.2. The rotating coordinate system is defined as $[x_I^f,\, y_I^f,\, z_I^f]$ and the inertial frame is defined as $[x_I,\, y_I,\, z_I]$. The interceptor fin frame fixed on the interceptor body is defined as $[x_m,\, y_m,\, z_m]$. The relative positions of the target with respect to interceptor in the rotating frame is given by

$$X_{rel} \triangleq [x_{rm}\; y_{rm}\; z_{rm}]^T \tag{12}$$

The relative velocity between interceptor and target is given by

$$\begin{bmatrix} \dot{x}_{rm} \\ \dot{y}_{rm} \\ \dot{z}_{rm} \end{bmatrix} = T_{IF} \begin{bmatrix} \dot{x}_t^I \\ \dot{y}_t^I \\ \dot{z}_t^I \end{bmatrix} - \begin{bmatrix} u \\ v \\ w \end{bmatrix} - \begin{bmatrix} qz_{rm} - ry_{rm} \\ rx_{rm} - pz_{rm} \\ py_{rm} - qx_{rm} \end{bmatrix} \tag{13}$$

Equation (13) is obtained by differentiating (12) such that derivative of the transformation matrix T_{IF} is given by [5]:

$$\dot{T}_{IF} = -\tilde{\omega}\; T_{IF},\;\; \tilde{\omega} = \begin{bmatrix} 0 & -r & q \\ r & 0 & -p \\ -q & p & 0 \end{bmatrix} \tag{14}$$

where $\tilde{\omega}$ is the skew-symmetric matrix.

III. PIGC: Mathematical Details

This section describes the implementation scheme of the PIGC.

A. Guidance (Outer Loop): MPSP

1) Generic Theory: In the MPSP technique, one needs to start from a "guess history" of the control solution. With the control guess history, obviously the objective will not meet, and hence, there is a need to improve the solution. In this section, we present a way to compute an error history of the control variable, which needs to be subtracted from the previous history to get an improved control history. A general nonlinear system is defined as

$$\dot{X} = f(X,U)$$

The discretized form of the state and output dynamics are

$$X_{k+1} = F_k(X_k,U_k),\;\; Y_k = h(X_k) \tag{15}$$

where $X \in \Re^n,\; U \in \Re^m,\; Y \in \Re^p$ and $k = 1,2,\ldots,N$ are the time steps.

$$X_{k+1} \;\; = \;\; X_k + \Delta t(f(X,U)) \tag{16}$$

However, from (15), we can write the error in state at time step $(k+1)$ as

$$dX_{k+1} = \left[\frac{\partial F_k}{\partial X_k}\right]\; dX_k + \left[\frac{\partial F_k}{\partial U_k}\right]\; dU_k \tag{17}$$

where dX_k and dU_k are the error of state and control at time step k respectively. The respective values for $\frac{\partial F_k}{\partial X_k}$ and $\frac{\partial F_k}{\partial U_k}$ are obtained from the discretized state model of (16). We aim for the output vector $Y_N \rightarrow Y_N^*$. Expanding Y_N about Y_N^* using Taylor series expansion and then using small error approximation we can write the error in the output, $\Delta Y_N \triangleq Y_N - Y_N^*$ as$\triangle Y_N \cong dY_N = \left[\frac{\partial Y_N}{\partial X_N}\right]\; dX_N$. The error in output obtained as:

$$dY_N = \left[\frac{\partial Y_N}{\partial X_N}\right]\left(\left[\frac{\partial F_{N-1}}{\partial X_{N-1}}\right] dX_{N-1} + \left[\frac{\partial F_{N-1}}{\partial U_{N-1}}\right] dU_{N-1}\right) \tag{18}$$

Similarly the error in state at time step $(N-1)$, dX_{N-1} can be expanded in terms of dX_{N-2} and dU_{N-2} and so on. Continuing the process until $k = 1$, we obtain

$$dY_N = B_1 dU_1 + B_2 dU_2 + \ldots + B_{N-1} dU_{N-1} = \sum_{k=1}^{N-1} B_k dU_k \tag{19}$$

assuming the error in the initial conditions is zero and it means $dX_1 = 0$. The key point is that the sensitivity matrices B_k is computed recursively which will save the computational time enormously [4]. In (19), we have $(N-1)m$ unknowns and p equations. Usually $p << (N-1)m$ and hence, it is an under-constrained system of equations. Hence, an additional objective is met by minimizing the following objective (cost function) subjected to the constraint in (19)

$$J = \frac{1}{2}\sum_{k=1}^{N-1}(U_k^0 - dU_k)^T R_k (U_k^0 - dU_k)$$

Here, U_k^0, $k = 1,\ldots,(N-1)$ is the previous control history solution and dU_k is the corresponding error in the control history. R_k is a positive definite matrices which is chosen judiciously by the control designer. After carrying out the necessary algebra [7] we get

$$dU_k = -R_k^{-1} B_k^T A_\lambda^{-1}(dY_N - b_\lambda) + U_k^0 \tag{20}$$

Hence, the updated control at time step $k = 1,2,\ldots,(N-1)$ is given by

$$U_k \;=\; U_k^0 - dU_k \tag{21}$$

One can refer to the details of MPSP technique in [4]

2) Mathematical Formulation: MPSP starts with the initial guess history which is generated from Proportional Navigation (PN) law off line. Curve fitting of the initial guess history obtained through PN law is done for the present study. It also provides the value for final time/time-to-go (t_f). MPSP algorithm works in two modes, namely the correction and prediction mode. In the correction mode, 9 states are considered given as $X \triangleq \begin{bmatrix} v & w & q_1 & q_2 & q_3 & q_4 & x_{rm} & y_{rm} & z_{rm} \end{bmatrix}^T$ Equations (4), (5), (6) and (13) are discretized using Euler Integration to get the discretized model [6]. Hence, the size of the matrix $\frac{\partial F_k}{\partial X_k}$ obtained in the present work is 9 by 9. The control for the outer loop formulation is the commanded pitch and yaw rate $U \triangleq \begin{bmatrix} q^* & r^* \end{bmatrix}^T$. Hence, the size of the matrix $\frac{\partial F_k}{\partial U_k}$ obtained is 9 by 2. The output of the MPSP is $Y_N \triangleq \begin{bmatrix} y_{rm} & z_{rm} & \dot{y}_{rm} & \dot{z}_{rm} \end{bmatrix}^T$. The desired output is $Y_N^* \triangleq \begin{bmatrix} 0 & 0 & 0 & 0 \end{bmatrix}^T$. In the prediction mode 17 states are considered as stated in (2) to predict the actual plant model. The convergence is obtained when the relative error in position and velocity of target and interceptor in y_I^f and z_I^f direction in fin frame as shown in Fig.2 decreases to a minimum specified value at t_f. The fin deflections are treated as time varying parameters in the correction mode of the MPSP formulation.

B. Control(Inner Loop) : Dynamic Inversion

The control loop is based on DI which ensures a good command tracking [8]. The fin deflection serves as the control for the inner loop and stabilizes the rotational dynamics. The error in commanded body rates and the actual body rates will generate fin deflections by enforcing the error dynamics. The commanded body rates are obtained from the guidance (MPSP) loop. The output vector for the inner loop is defined as $Y = \begin{bmatrix} p & q & r \end{bmatrix}^T$ and the control vector is $U_\delta = \begin{bmatrix} \delta_r & \delta_p & \delta_y \end{bmatrix}^T$. The governing state model for inner loop contains only the body rates. The DI formulation results in a square system (no. of outputs same as number of inputs) [8]. The control explicitly appears in the first order derivative of the output variable in the inner loop. Thus,

$$\dot{Y} = f_y(X) + g_y(X)U \tag{22}$$

The goal is $Y \rightarrow Y^*$, where $Y^* = [p^* \quad q^* \quad r^*]^T$. The error of tracking is defined as $E \triangleq Y(t) - Y^*(t)$. Enforcing the first order error dynamics, such that $E \rightarrow 0$ as $t \rightarrow \infty$. Here, $ki = diag(\frac{1}{\tau})$ and $\tau = T_s/4$ is the time constant of the first order system. It is selected based on the small settling time ($T_s = 0.4sec$) due to the fast nature of the rotational dynamics.

$$U_\delta = [g_y(X)]^{-1}[-(f_y(X) - \dot{Y^*}) - K(Y - Y^*)] \tag{23}$$

The updated value of fin deflections U_δ is used for propagation of system dynamics. The inner loop assures the convergence of the body rates to their desired/commanded values obtained from the guidance loop such that $q \rightarrow q^*$ and $r \rightarrow r^*$. In this way, the rotational dynamics will only be responsible for generating the effective control (fin deflections) and no over coupling with translational dynamics is accounted which was happening earlier in IGC design.

IV. Simulation Results

For our simulation studies, a surface to air interceptor is considered which is aiming for a high speed threat in terminal homing. Both the target and interceptor model equations are simulated by using Runge-Kutta method to get the required knowledge of the updated plant dynamics trajectory [6]. The guidance cycle is $12.5msec$ and the state update cycle is $2.5msec$. The time of engagement (t_f) is $3.9973sec$. Assuming the lethal range of $5m$, we got the final miss distance less than $0.5m$. Results appears to be promising in context with the zero effort miss (ZEM) which is around $500m$. It is the distance by which the interceptor will miss the target if it continues along its present course with no control applied by the interceptor.

A. Comparison between Three-Loop (Conventional) Design and PIGC

In conventional systems, guidance and control subsystems are designed separately and then integrated together into the missile. The performance of such systems are not optimized truely. The logic of PIGC is validated by carrying out the comparative study with the conventional design. We can observe from the Fig. 3, that the commanded body rates has a straight line profile compared to that of PN law used in the conventional design. This comes with the advantage of natural stabilization of the missile body with faster correction of miss distance. Figure 4 shows the control fins getting saturated in case of PN law compared to the case of PIGC. It shows that the objective of minimum distance with minimum control effort is met. The control values are much below their saturation limits. To get the miss distance of the same order,

conventional design uses the maximum fin deflection and finally goes into saturation as shown in Table.I.

TABLE I

SIMULATION RESULTS FOR DIFFERENT INITIAL CONDITIONS

Cases	Zero Effort Miss (m) (with no control)	Miss distance(m) (Three-Loop Design)	Miss distance(m) (PIGC Design)
1	627.71	2.135	1.018
2	558.05	2.655	0.759
3	522.80	2.060	0.748
4	649.17	0.699	0.509
5	692.50	2.341	0.552

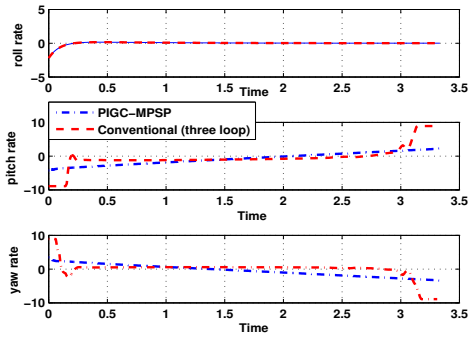

Fig. 3. Comparison between conventional three loop design and PIGC

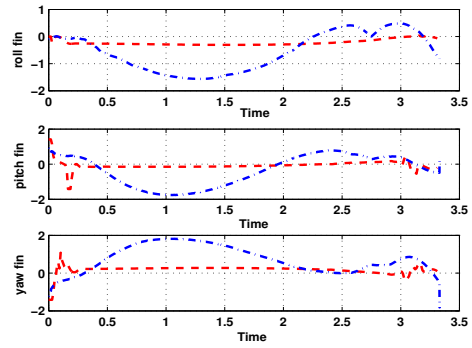

Fig. 4. Comparison between conventional three loop design and PIGC

B. Comparison between One-Loop IGC Design and PIGC

In a One-Loop design, the guidance law and autopilot design are formulated into a single unified state space framework. A comparative study has also been carried out between State dependent Ricatti Equation (SDRE) based one loop IGC design and PIGC approach[3]. Table II shows the comparative study of one loop IGC and PIGC in terms of miss distance and zero effort miss for different cases. It is evident from Table II that the engagement in PIGC takes place at a miss distance of the order of less than $0.2m$. All the results are normalized trajectories. Figure 5 shows the $3D$ engagement scenario in inertial frame of PIGC scheme. Figure 6 represents the magnified view of

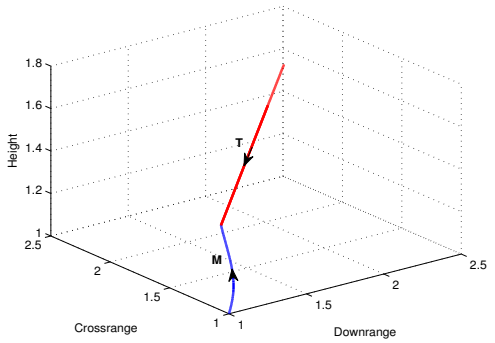

Fig. 5. Engagement in 3D space for PIGC.

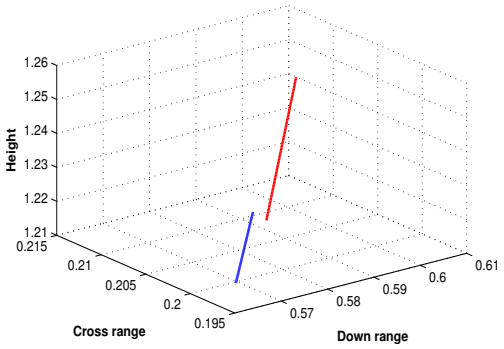

Fig. 6. Magnified view in 3D space for One-loop IGC

$3D$ engagement geometry in case of one loop IGC. It is also seen in Table II that the objective of minimum distance is not met. Figure 7 shows the comparative plot of body rates of conventional IGC and PIGC scheme. Figure 8 represents the comparative plot of fin deflections obtained through SDRE and DI controller in PIGC scheme.

TABLE II

SIMULATION RESULTS FOR DIFFERENT INITIAL CONDITIONS

Cases	Zero Effort Miss(m) (with no control)	Miss Distance(m) (One-Loop IGC)	Miss Distance(m) (PIGC)
1	55.27	39.767	0.0348
2	53.17	32.147	0.1714
3	27.05	11.88	0.2481
4	50.49	24.85	0.1097
5	44.82	14.56	0.2167

C. Simulation Study with Different Initial Condition

Different cases were studied with interceptor and target initial state perturbations to check the effectiveness of the PIGC scheme. Body rates were perturbed differently, with roll rate (p) between $\pm 20^o$, pitch rate (q) and yaw rate (r) between $\pm 10^o$. Random deviation of 2% is considered for both interceptor and target initial conditions together. Figure 9 shows the family of trajectories of $3D$ engagement. Figures 10 and 11 represents the body rates and fin deflections of the interceptor.

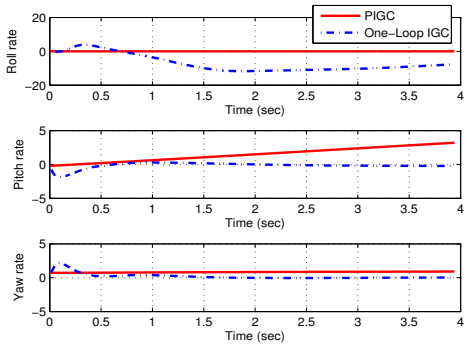

Fig. 7. Body rates

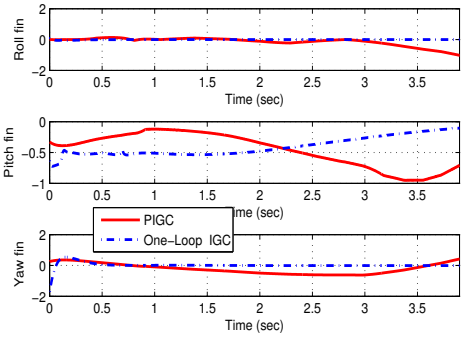

Fig. 8. Control deflections

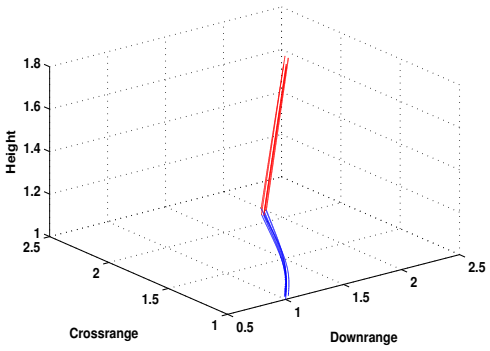

Fig. 9. Engagement Geometry from various initial conditions

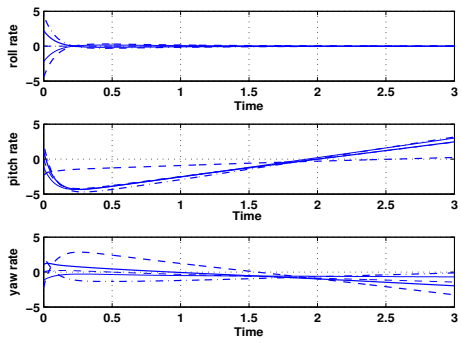

Fig. 10. Body rates of the interceptor

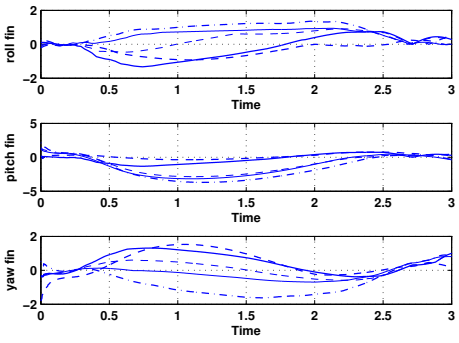

Fig. 11. Fin Deflection of the interceptor

V. Conclusion

Using powerful nonlinear and optimal control design methods like MPSP and dynamic inversion, this paper proposes a new philosophy of partial integrated guidance and control scheme for high speed targets in the terminal homing loop of interceptors. The newly proposed PIGC algorithm yields smaller miss distance with minimum control effort. PIGC scheme uses Six-DOF nonlinear model for both guidance and control loop. This intelligent manipulation preserves the inherent time scale separation property between the translational and rotational dynamics, and hence overcomes the deficiency of current IGC designs. However, it preserves the benefits of the IGC philosophy. Comparative studies of the proposed PIGC scheme with three loop conventional design and one loop IGC has also been performed. Simulations with different initial conditions shows the advantages of the PIGC scheme. The final miss distance is well within the lethal range.

References

[1] G. M. Siouris, “Missile Guidance and Control Systems”, Springer, Inc NetLibrary 2004.

[2] P. K. Mennon, E. J. Ohlmeyer, “Nonlinear Integrated Guidance-Control Laws for Homing missiles”, AAIA Guidance, Navigation and Control Conference and Exhibit 6-9 August 2001, Montreal, Canada.

[3] N. F. Palumbo, T. D. Jackson, “Integrated Guidance and Control: A State Dependent Ricatti Differential Equation Approach”, IEEE International Conference on control Applications, Piscataway, NJ, 1999.

[4] R. Padhi and M. Kothari, “Model Predictive Static Programming: A Computaionally Efficient Technique for suboptimal control Design”, International Journal of Innovative Computing,Information and Control, Vol.5, No.2, February 2009.

[5] H. Schaub and J. L. Junkins, “Analytical Mechanics of Space Systems,” AIAA Education Series, 2003.

[6] K. E. Atkinson, “An Introduction to Numerical Analysis,” Jhon Wiley & Sons, 2001.

[7] A. E. Bryson and Y. C. Ho, “Applied Optimal Control”, Hemisphere Publishing Corporation, 1975.

[8] D. Enns, D. Bugajski, R. Hendrick and G. Stein, “Dynamic Inversion: an evolving methodology for flight control design,” International Journal of Control, Vol.59, No.1, pp. 71-91, 1994.